Journal of Experimental Botany, Vol. 62, No. 6, pp. 2179–2188, 2011
doi:10.1093/jxb/erq418 Advance Access publication 5 January, 2011
This paper is available online free of all access charges (see http://jxb.oxfordjournals.org/open_access.html for further details)

Journal of Experimental Botany
www.jxb.oxfordjournals.org

RESEARCH PAPER

Visualization of lateral water transport pathways in soybean by a time of flight-secondary ion mass spectrometry cryo-system

Morio Iijima[1,*], Tomoharu Yoshida[2], Toshiyuki Kato[2], Michio Kawasaki[3], Takamasa Watanabe[2] and Sutharsan Somasundaram[2,4]

[1] School of Agriculture, Kinki University, Nara 631-8505, Japan
[2] Graduate School of Bioagricultural Sciences, Nagoya University, Nagoya 464-8601, Japan
[3] Faculty of Agriculture and Life Science, Hirosaki University, Aomori 036-8561, Japan
[4] Faculty of Agriculture, Eastern University Sri Lanka, Chenkalady 30350, Sri Lanka

* To whom correspondence should be addressed. E-mail: iijimamorio@nara.kindai.ac.jp

Received 14 August 2010; Revised 16 November 2010; Accepted 25 November 2010

Abstract

Water movement between cells in a plant body is the basic phenomenon of plant solute transport; however, it has not been well documented due to limitations in observational techniques. This paper reports a visualization technique to observe water movement among plant cells in different tissues using a time of flight-secondary ion mass spectrometry (Tof-SIMS) cryo-system. The specific purpose of this study is to examine the route of water supply from xylem to stem tissues. The maximum resolution of Tof-SIMS imaging was 1.8 μm (defined as the three pixel step length), which allowed detection of water movement at the cellular level. Deuterium-labelled water was found in xylem vessels in the stem 2.5 min after the uptake of labelled water by soybean plants. The water moved from the xylem to the phloem, cambium, and cortex tissues within 30–60 min after water absorption. Deuterium ion counts in the phloem complex were slightly higher than those in the cortex and cambium tissue seen in enlarged images of stem cell tissue during high transpiration. However, deuterium ion counts in the phloem were lower than those in the cambium at night with no evaporative demand. These results indicate that the stem tissues do not receive water directly from the xylem, but rather from the phloem, during high evaporative demand. In contrast, xylem water would be directly supplied to the growing sink during the night without evaporative demand.

Key words: Deuterium, *Glycine max* (L.) Merr. Münch's counterflow, pressure–flow hypothesis, soybean, time of flight-secondary ion mass spectrometry, water recycling, water uptake.

Introduction

Soil water absorbed by crop roots is mainly transported through the xylem to stem tissue by transpirational pull. During sunny days, most of the absorbed water is lost by transpiration and only some of the water is used for cell enlargement and metabolism. According to Münch's hypothesis (1930), a fraction of the transported water in the xylem would flow into the phloem tissue in leaves and would be used for pressure flow. In other words, a fraction of absorbed soil water has been hypothesized to be redistributed to the cells in roots and stems through phloem tissue. This has been studied extensively (e.g. Hölttä *et al.*, 2006*a*, *b*), but only limited evidence (such as Windt *et al.*, 2006) has been reported so far due to the difficulties in the experimental technique. Due to the lack of quantitative evidence of water movement among plant cells, it is not known whether soil water is mainly supplied to the growing cells in the plant body by the xylem or the phloem tissue.

Experimental techniques such as stem flow measurement (Higuchi and Sakuratani, 2006; Helfter *et al.*, 2007), dye tracer method (Varney *et al.*, 1993; Sano *et al.*, 2005; Keller

et al., 2006), hydrostatic pressure measurement (Gould et al., 2004, 2005), neutron beam analysis (Nakanishi et al., 2003), and the latest nuclear magnetic resonance imaging (MRI) (Peuke et al., 2006; Windt et al., 2006; Van As, 2007; Scheenen et al., 2007) have been used to observe water movements in plant bodies. These techniques make it possible to analyse not only the water flow inside the vascular bundle tissues but also plant water uptake. For example, an apoplastic tracer dye is an indicator of plant water uptake; water fluxes can be estimated by the rate of accumulation of dye (sulphorhodamine G) at the root surface (Varney and Canny, 1993). The symplastic pathway for water transport can also be evaluated by the dye concentration in the cells in each tissue (Varney et al., 1993). The xylem-mobile dye basic fuchsin has been widely used to monitor xylem flow (for example by Keller et al., 2006), and phloem transport has been investigated by the use of Oregon Green (Liu and Gaskin, 2004).

MRI techniques are now used to study the water flow of plant species in addition to obtaining anatomical information (Van As, 2007). For example, this technique can be used to determine the diurnal changes in flow-conducting areas of phloem and xylem (Windt et al., 2006; Scheenen et al., 2007). Although MRI techniques have been used to visualize plant water status, their resolution is generally not high enough to examine the structures of xylem and phloem pathways (Windt et al., 2007).

Water movement from phloem cells to growing parenchyma cells is not easy to detect by the techniques discussed above. The dye tracer method is limited to the apoplastic water uptake or water movement along xylem or phloem tissues because the dye will not move from the vascular tissues to the parenchyma tissues. Currently, the best possible resolution of the MRI microscopic technique to analyse the lateral water movement among different tissue levels is ~14 μm (Köckenberger et al., 2004), except for the analysis of high resolution lipid distribution images of 6 μm, which requires trimming of the sample plane to the dimensions of the micro-coil (Fig. 7 of Schneider et al., 2003). Although a cellular level of imaging was possible by this technique (eg. Van As 2007; Sibgatullin et al., 2010), imaging of water movement between the xylem (and/or phloem) and growing cells may be difficult. A much higher resolution technique to trace the water movement is necessary for detailed analysis of water movement, such as that posited by Münch's counterflow hypothesis (water movement from xylem to phloem).

This paper describes a technique to visualize water movement from xylem to stem parenchyma cells by a time of flight-secondary ion mass spectrometry (Tof-SIMS) cryo-system. Tof-SIMS determines the surface chemical structure as the positional image and/or mass spectrum information. When a pulsed primary ion beam is bombarded onto the surface of a solid specimen, the secondary ions from the top 2–3 atomic layers (10–20 Å) are emitted from the surface and are detected as the positional image. The maximum resolution for the positional image of Tof-SIMS used in the present study was 1.8 μm (defined as a three pixel step length to distinguish two separate dots); thus, it was possible to perform cellular level analysis once the surface structure of the plant was rigid enough under a high vacuum. Tof-SIMS has been used to identify the surface constituents of non-organic materials (e.g. semiconductors), but recently it was also used to analyse organic materials such as lignin polymer (Saito et al., 2005a, b, 2006), pulp fibre (Matsushita et al., 2005, 2007), and heartwood tissue (Imai et al., 2005; Tokareva et al., 2007). Tof-SIMS requires a high vacuum to observe the surface structure, and thus is limited in its ability to analyse water-rich materials such as herbaceous annual crop species; it can be applied only to dried wood materials, which will not be disturbed under high vacuum conditions. Recently, a Tof-SIMS instrument equipped with a cryo-stage was used for the analysis of macronutrients in plants (Metzner et al., 2008) and inorganic materials (Nair et al., 2004), which are difficult to analyse under high vacuum environments without surface treatments of water-rich and/or volatile compounds. Metzner et al. (2008) first traced the transport routes of macronutrients in plants at the level of cells and tissues and measured their chemical distributions. Just very recently they also reported the dynamics of water and mineral nutrients in bean stem tissue using $H_2^{18}O$ and D_2O as the stable isotope for water (Metzner et al., 2010). A similar techniques was used here to trace the water itself, using deuterium-labelled water as the tracer. The specific purpose of this study is to examine the route of water supply from xylem to stem parenchyma cells by a technique to visualize the cellular level of water movement using a cryo-Tof-SIMS.

Materials and methods

Plant growth

As the test plant for this study, a soybean [*Glycine max* (L.) Merr.] cultivar, 'Fukuyutaka' which is widely cultivated and is a recommended commercial cultivar in Japan, was used. Pre-germinated seeds (in darkness at 30 °C for 60 h) in a Petri dish were grown in an aerated water culture (container size, 20×19×16 cm; volume, 6.0 l) for 14 d up to the second and third leaf stage inside a growth chamber (16 h day length, 30 °C during the day and 25 °C during the night). At this stage soybean stem shows rapid secondary expansion growth, and therefore it should be easy to detect water movement from roots to growing parenchyma cells in the stem.

Deuterium uptake and sample preparation

Deuterated (heavy) water was used as the tracer for plant water uptake (Ijima et al., 2007; Zegada-Lizarazu et al., 2007). At 14 d after planting, plants were transferred to the aerated water culture with 99.9 atom% deuterium-labelled water (D_2O). In experiment 1, the deuterium labelling was conducted during the morning, starting from 09:00–10:00 h on sunny days with photosynthetically active solar radiation of 1300–1400 μmol m^{-2} s^{-1} at 30–32 °C inside an open glasshouse with good ventilation. The relative humidity was ~53–67% during the experiment. Plants were harvested at 1, 2.5, 30, 60, and 120 min after transfer. In experiment 2, the deuterium labelling was conducted inside the growth chamber (30 °C during the day and 25°C during the night) during the afternoon starting from 13:00 h and continued up to

sunset hours (4 h of labelling, harvested at 17:00 h just before the night period starts) or night hours (8 h of labelling, harvested at 21:00 h) inside the growth chamber. The plant shoot samples of ~4 cm length and 2 mm diameter were quickly excised with a scalpel blade below the cotyledon and were rapidly shock-frozen by plunging into liquid nitrogen (–196 °C). Frozen shoot samples were kept in a deep freezer at –85 °C until sectioning. Clean and even surfaces, as needed for ToF-SIMS analysis, were obtained by sectioning the samples with a cryo-microtome (OT/FAS; Bright Co. Ltd, UK) at –20 °C. Frozen samples were quickly moved into the cryo-chamber for sectioning. The cryo-sectioning procedure did not cause the visible local thawing of the soybean young stem samples judging from the Tof-SIMS images used for the present study. Samples of 30 μm thickness were mounted on a silicon plate with the aid of carbon tape and again kept in the deep freezer until ToF-SIMS measurement.

Cryo-Tof-SIMS measurement

Analysis was conducted using a Tof-SIMS spectrometer (TRIFT III; ULVAC-PHI Co. Ltd, Japan) equipped with a cryo-stage (Physical Electronics Co. Ltd).

Mass resolution at the deuterium peak (2.027 *m/z*) was 8000. Samples were fixed in a cryo-holder immersed in liquid nitrogen and then inserted into a sample chamber maintained below –130 °C. The chamber vacuum was kept below 1×10^{-5} Pa after transfer and operated with a pulsed mass-filtered 22 keV Au_1^+ primary ion beam at a raster size of 200×200 μm (for surface analysis) or 150×150 μm (for enlarged image analysis). The pulse frequency was 8430 Hz and pulse duration was 15.18 ns. Primary ion current for the measurement was DC 600 pA. The total ion counts were $>2.0\times10^6$ for both spectrum and image analysis. Accumulation of $>3.0\times10^6$ total ions did not improve the images of deuterium distribution (data not shown). Ion accumulation took ~5–15 min depending on the sample conditions. Only negatively charged ions were analysed for the deuterium ion peak. The measurement was conducted in the static SIMS mode. Total doses were 3.34×10^{11}–1.78×10^{12} ions cm^{-2}. Similar conditions were used in the studies analysing the plant materials by the same Tof-SIMS set-up published elsewhere (eg. Imai *et al.*, 2005; Matsushita *et al.*, 2005, 2007; Saito *et al.* 2005*a*, *b*, 2006). The theoretical resolution depends on the beam size used for the cryo-Tof-SIMS analysis. A beam size of 0.3 μm was used, and the maximum pixel step size was 0.59 μm in the enlarged images. Following the resolution concept, the actual resolution of the present work was defined as three pixel step length=1.77 μm to distinguish two separate dots at maximum in order to observe the lateral water transport of young soybean stem sections.

Bright-field microscopy

The semi-ultrathin sections of stems were observed with a bright field microscope to identify the tissue structure in the Tof-SIMS images. The samples were excised from about the same positions in the stems. The segments were fixed in 0.05 M sodium phosphate buffer (pH 7.2) containing 1% glutaraldehyde and 2% paraformaldehyde at 20 °C for 5 h. They were washed with 0.1 M sodium phosphate buffer, and post-fixed in 0.1 M sodium phosphate buffer containing 1% osmium tetroxide at 4 °C for 8 h. Fixed samples were dehydrated through a graded series of acetone and permeated by propylene oxide. The samples were then embedded in Spurr's resin and polymerized at 70 °C for 24 h. Semi-ultrathin sections (1 μm in thickness) were cut with a glass knife on an ultramicrotome (EM UC6; Reichert). Sections were stained with toluidine blue O and observed with a bright field microscope (BX51; Olympus).

Scanning electron microscopy

Frozen samples of the soybean stems were also observed with a scanning electron microscope (low-vacuum reflection electron method; Natural SEM/WET-SEM; S-3000N Hitachi) to identify the tissue structures in the Tof-SIMS images. The samples were imaged at an acceleration voltage of 1.50 keV at a stage temperature below –20 °C and a pressure of 30 Pa.

Quantification of deuterium ions

Accumulation of deuterium ions in each tissue was quantified to analyse the water flux from the root to the stem. The deuterium ion counts in cells of different stem tissues, which can be clearly identified within the field of view, were all analysed by the Win Cadence Tof-SIMS software (ULVAC-PHI). The cells or regions in each tissue, which can be easily identified in the images of total ions, were manually selected and the deuterium ion counts of selected area were measured. The values were expressed as the average number of deuterium ion counts per 1 μm^2 of cells in each tissue.

Statistical analysis

In total 38 plants and 56 samples were used for the surface analysis from >200 soybean plants grown for this study. Fisher's protected least-significant difference (PLSD; a post-hoc test) test was used for the comparisons of the secondary ion counts per unit area of the Tof-SIMS images among the different tissues. At least three replicates plants were observed for each analysis of the time course measurements in both experiment 1 and 2. The number of observations for the statistical analysis was from four (two replicate plants×two different positions in stem) to eight (three replicate plants×two–three different positions in the stem).

Results and Discussion

Water distribution pathways from plant roots to the growing cells have not been well documented so far due to the experimental difficulties in tracing water movement along vascular tissues to parenchyma cells. It may be directly distributed from xylem vessels to the parenchyma cells or it may be distributed through phloem counter-flow as hypothesized by Münch (1930). This study presented the visual and circumstantial evidence for both day and night by the use of cryo-Tof-SIMS.

Validity of secondary ion spectra

ToF-SIMS analysis of deuterium-labelled water movement requires verification of the absorption of secondary ions of

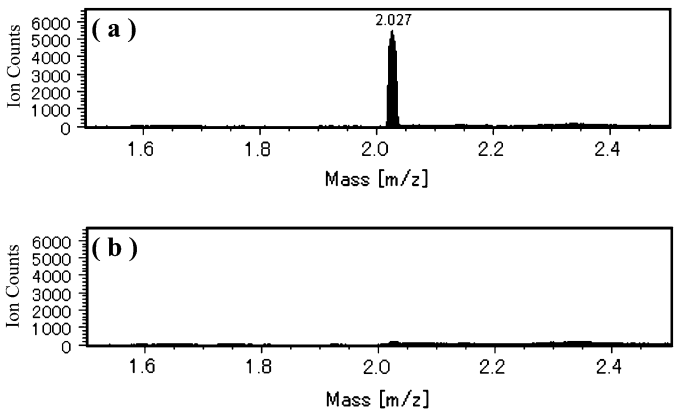

Fig. 1. Comparison of secondary ion spectra. Negative ToF-SIMS spectra (*m/z*=1.5–2.5) acquired from a soybean stem section: (a) application of D_2O; (b) application of H_2O.

deuterium by plants. Negative ion mass spectra ranged from 1.5 to 2.5 *m*/*z* by Tof-SIMS of the plant samples with deuterium-labelled water and non-labelled water, as shown in Fig. 1. The deuterium ion peak (2.027) was found in the deuterium-labelled sample (60 min deuterium absorption), while none was found in the non-labelled sample. The total ion count of this peak (within 1.5–2.5 *m*/*z*) was 60 000 for the labelled water and 2000 for non-labelled water. This indicates that the deuterium ion peak represents the uptake of deuterium-labelled water. Nearly 30 times higher accumulation of deuterium ions as compared with the control was found in the 60 min deuterium ion labelling. Previous studies on deuterium labelling of crop species indicated that plant xylem sap contains 0.05–0.902 atom% excess deuterium concentrations in various agricultural field and/or pot experiments (e.g. Zegada-Lizarazu and Iijima, 2004, 2005; Araki and Iijima, 2005; Iijima *et al.*, 2005; Zegada-Lizarazu *et al.*, 2005, 2006*a*, *b*; Iijima *et al.*, 2007). These values mean that the deuterium labelling was only 4–58 times higher than the unlabelled control condition (the natural abundance of deuterated water was ~0.0156% on average of the soil water). This agreed well with the present value of 30 times higher deuterium accumulation in the 60 min samples. Much longer absorption in experiment 2 (8 h D_2O absorption) did not significantly improve the deuterium accumulation in the image. In this study, the number of total pixels in each image was fixed as 65 536 (256×256). Therefore, 60 000 deuterium ion counts in total in each field of view means that there were 0.92 deuterium ion counts per pixel on average. At maximum, 10 (Figs 3, 4) deuterium ion counts per pixel was good enough to analyse the deuterium accumulation because only 30.5 total ions exist in each pixel

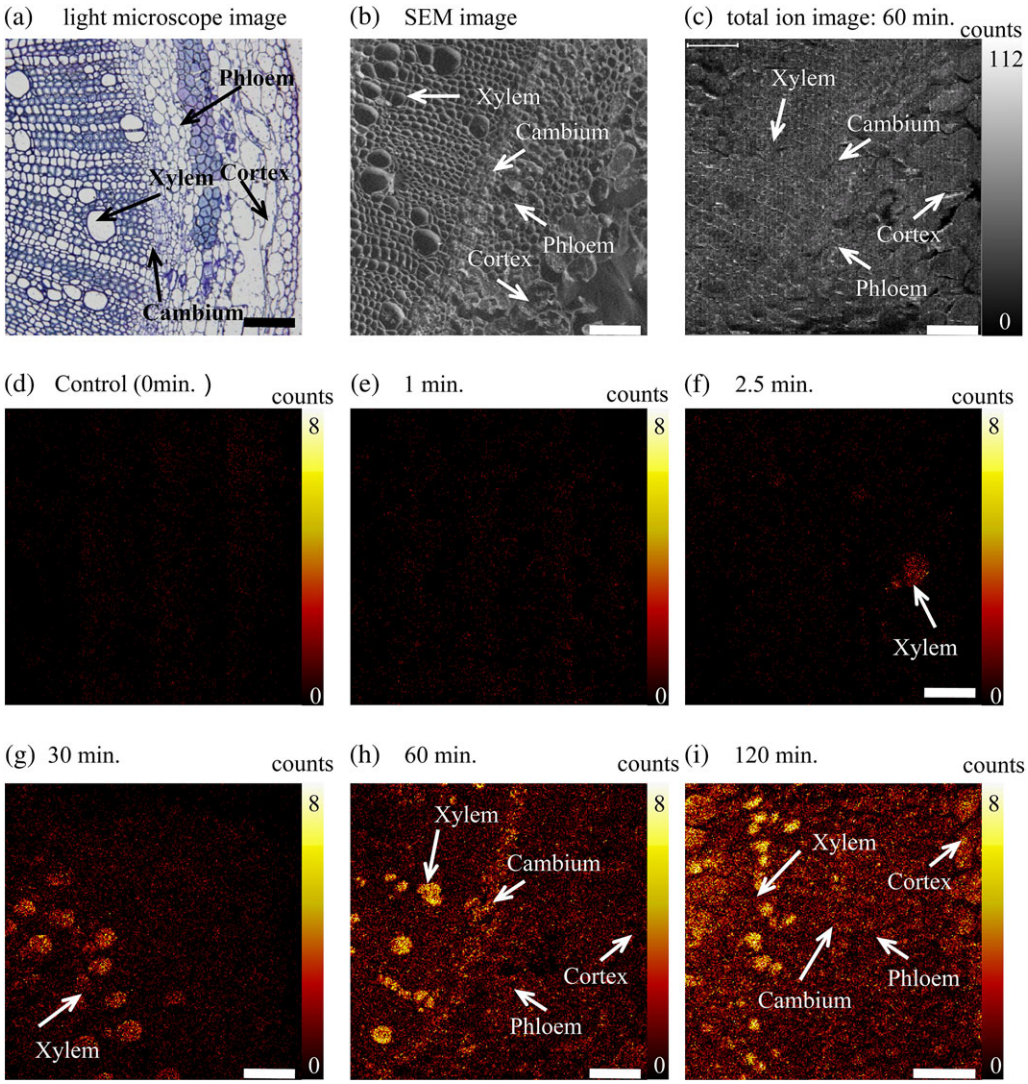

Fig. 2. Time-course changes in D_2O distribution in stem tissue under high evaporative demand (experiment 1). (a) Semi-ultrathin section of a soybean stem; (b) scanning electron microscopy image; (c) total ion accumulation of the Tof-SIMS cryo-system; (d–i) ToF-SIMS deuterium ion images. The time elapsed after D_2O application is shown in each image. The resolutions of ToF-SIMS images (defined as three pixel step length herein) are 5.9 μm in (d), (e), and (i), and 7.0 μm in (f–h). Scale bar (lower right in each figure)=100 μm. The coloured bars (right side) indicate the intensity of the secondary ions. Black indicates the lowest intensity and white indicates the highest intensity.

on average (measurement was continued until 2.0×10^6 ions accumulated in each image).

Water absorption

Time-course changes in D_2O distribution in stem tissue are shown in Fig. 2. Deuterium ions which did not originate from the deuterated water are indicated in the control image (Fig. 2d), which was sampled just before the deuterium labeling; in other words 0 min sampling. The image indicates the natural abundance of deuterium ions (~0.0156%) accumulated in the soybean plant body. All the replicate images showed very similar trends in terms of the presence of deuterium. Semi-ultrathin sections (Fig. 2a) and scanning electron microscopy images (Fig. 2b) in a similar region of the total secondary ion image (Fig. 2c) are shown to support the anatomical information provided by the Tof-SIMS analysis. Samples taken at 1 min after heavy water absorption (Fig. 2e) did not show any particular deuterium presence; they were similar to the control image. At 2.5 min after heavy water absorption (Fig. 2f), deuterium ions began accumulating in one of the xylem vessels (judging from the total ion accumulation image) and were visible in many of the xylem vessels at 30 min after deuterium uptake (Fig. 2g). The presence of deuterium ions was evident in the cambium and phloem tissues at 60 min (Fig. 2h) and in cortex tissues at 120 min after uptake. Deuterium uptake was clearly indicated at the tissue level with the time-course sampling.

Deuterium distribution among tissues

The details of water distribution among stem tissues during high evaporative demand (experiment 1) were analysed in an enlarged image (Fig. 3). The specific resolution (three pixel step size) was 1.8 μm at the maximum enlargement of an image field (150×150 μm). In soybean stem, the size of phloem tissue varied significantly; one sample in this image was extremely large compared with another one in the micrograph. Images in Fig. 3a, b, and d are not from the same sections, because of the difficulty of sample preparation with the present technique. Judging from the position

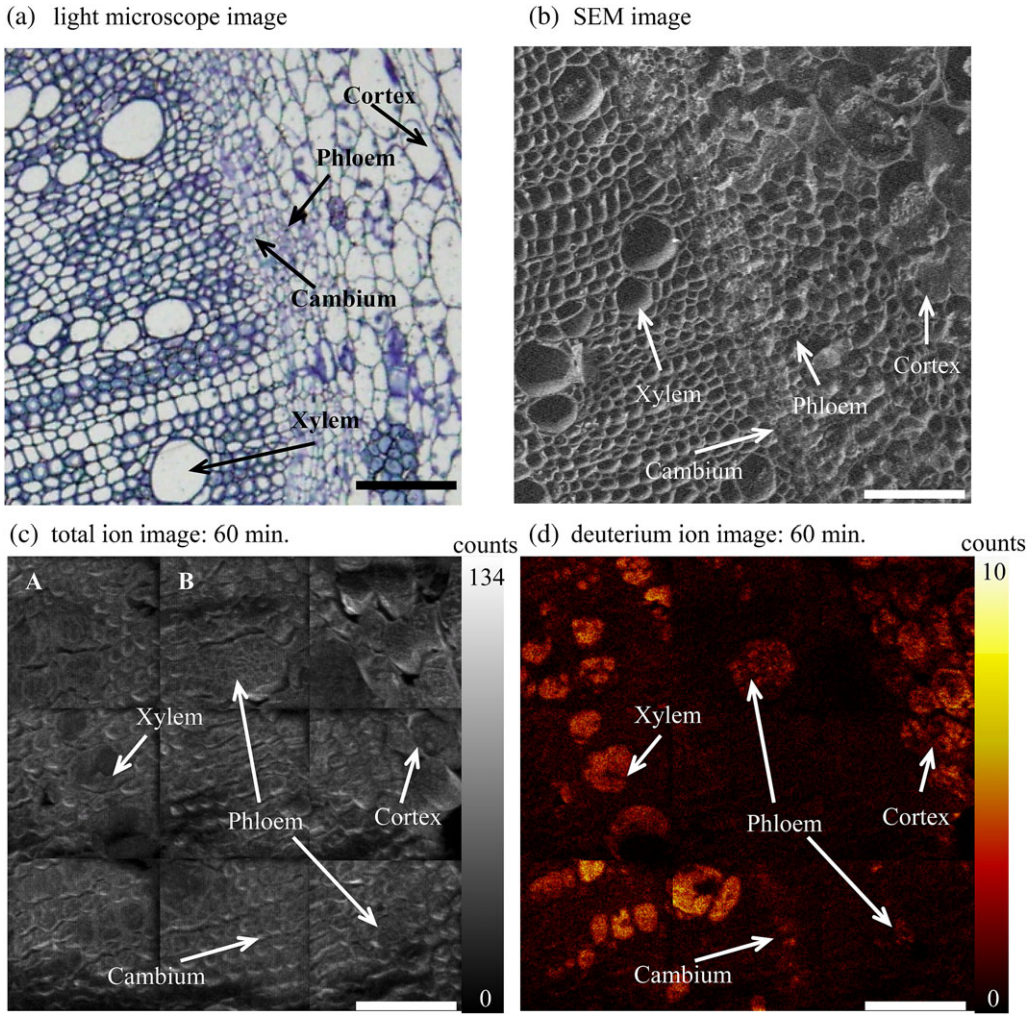

Fig. 3. Distribution of D_2O in soybean stem tissue under high evaporative demand (experiment 1). The specific resolution of ToF-SIMS images is 1.8 μm (three pixel step size). Scale bar (lower right in each figure)=100 μm. The coloured bars (right side) indicate the intensity of secondary ions. Black indicates the lowest intensity and white indicates the highest intensity. In A (xylem parenchyma region) and B (phloem parenchyma region) of the total ion image, the line scan is shown in Fig. 4.

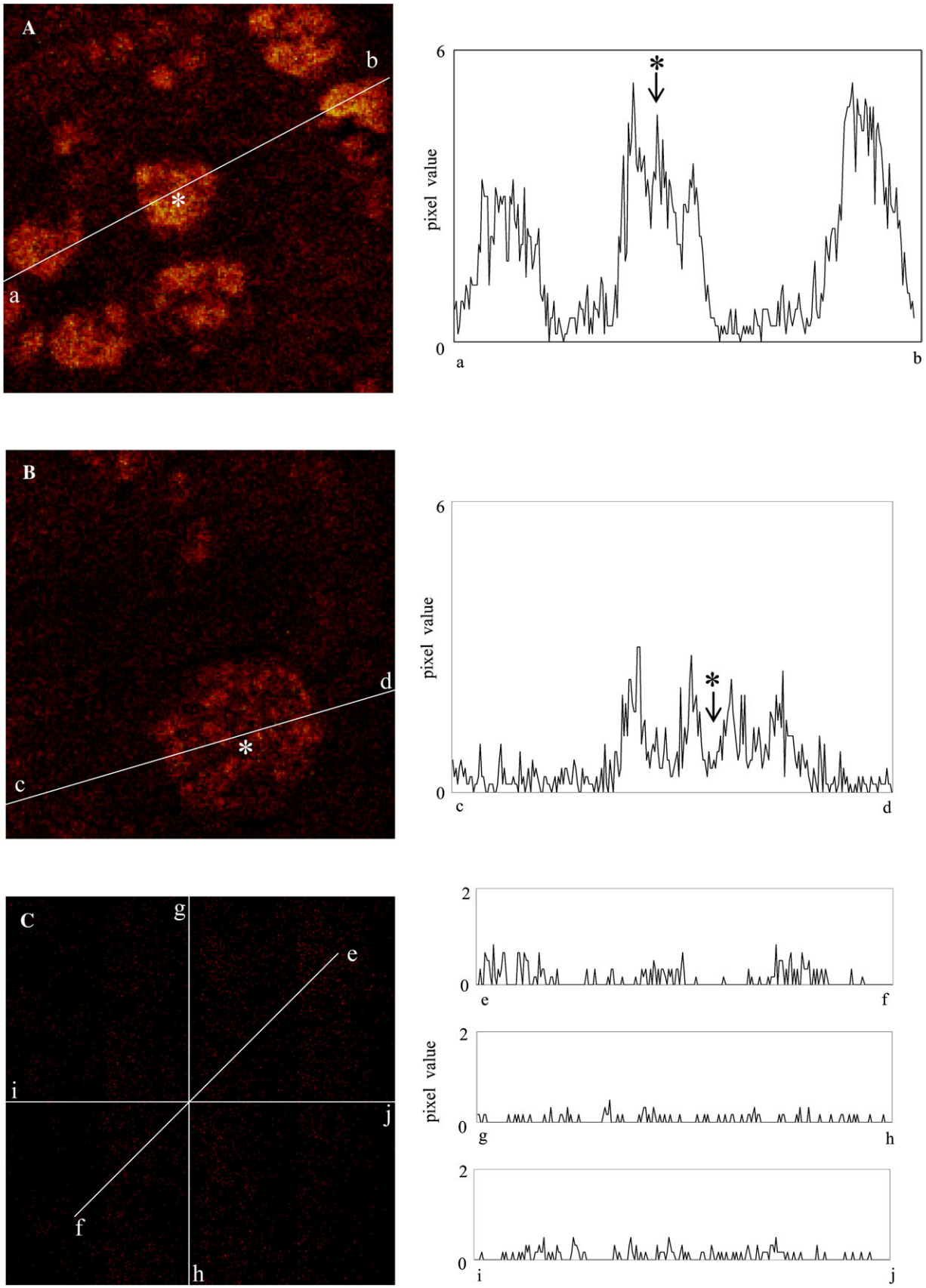

Fig. 4. Line scan of xylem (A), phloem (B), and control (C). A and B deuterium images are the enlarged images from Fig. 3d, and C is the control (deuterium non-labelling) sample from Fig. 2d. The line scan was computed from the image data set of the deuterium images along the path from a to b (upper), c to d (middle), and e–f, g–h, i–j (lower). The centre part of the largest xylem and phloem vessels in the line is marked in both figures by an asterisk (*).

and the shape of these tissues in both Fig. 3c and d, it is concluded that both of them indicated by arrows are the phloem tissues. The water movement among vascular tissues and fundamental tissues was clearly evident in the enlarged image; deuterium ion signals were evident inside the xylem and phloem vessels and in cortical and cambium cells. In contrast, deuterium ion accumulation in the xylem and phloem parenchyma cells and the apoplastic region among the cortical cells was not found in the enlarged image. However, the movement of water by mere diffusion from xylem to phloem and other neighbouring tissues may occur during the 60 min of the experiments. Therefore, the line scanning of xylem and phloem parenchyma cells, and control images was conducted to check the deuterium levels around the vascular system. Line scanning in both the xylem and phloem parenchyma region indicated that slightly higher deuterium signals were evident in the apoplastic and/or symplastic region as compared with the absolute control value (Fig. 4). This implied that the slight movement of deuterium water by the diffusion from both xylem and phloem tissue occurred. Figure 5 shows the deuterium distribution among stem tissues during less (sunset) or no (night) evaporative demand (experiment 2). Both 4 h (Fig. 5c, d) and 8 h (Fig. 5e, f) of D_2O absorption produced deuterium accumulation in parenchyma tissues, although the deuterium signal did not differ (maximum 10 counts per pixel) from 1 h labelling in Experiment 1. A longer labelling time may have caused much more absorption of deuterium water by parenchyma cells. These images showed basically similar trends during high evaporative demand. At sunset sampling, deuterium ions accumulated in cambium tissue which would be actively growing during the afternoon period. In contrast, deuterium ions accumulated in phloem tissues at night. These phenomenon are discussed in the next section.

Visual evidence of water supply from the xylem to stem parenchyma cells

Quantification of deuterium ions in an image would provide information on how water was sequentially distributed within the stem tissue. The deuterium ion counts can be regarded as the quantitative information of water flux. The distribution of deuterium ions in each tissue was quantified in both experiments (Table 1). In the enlarged image of the stem cell tissue, deuterium ion counts in the xylem vessels were significantly higher than in other tissues, and those in the phloem complex were slightly higher than those of the cortex and cambium tissue under high evaporative demand. The quantification of deuterium ion counts suggested the sequence of water movement from xylem to other tissues; xylem water was distributed to phloem first, and then water moved to the cambium and cortex tissues. The absorbed water from the root together with photosynthetically fixed sucrose must be distributed to the stem parenchyma cells via phloem in the young soybean stem when the evaporative

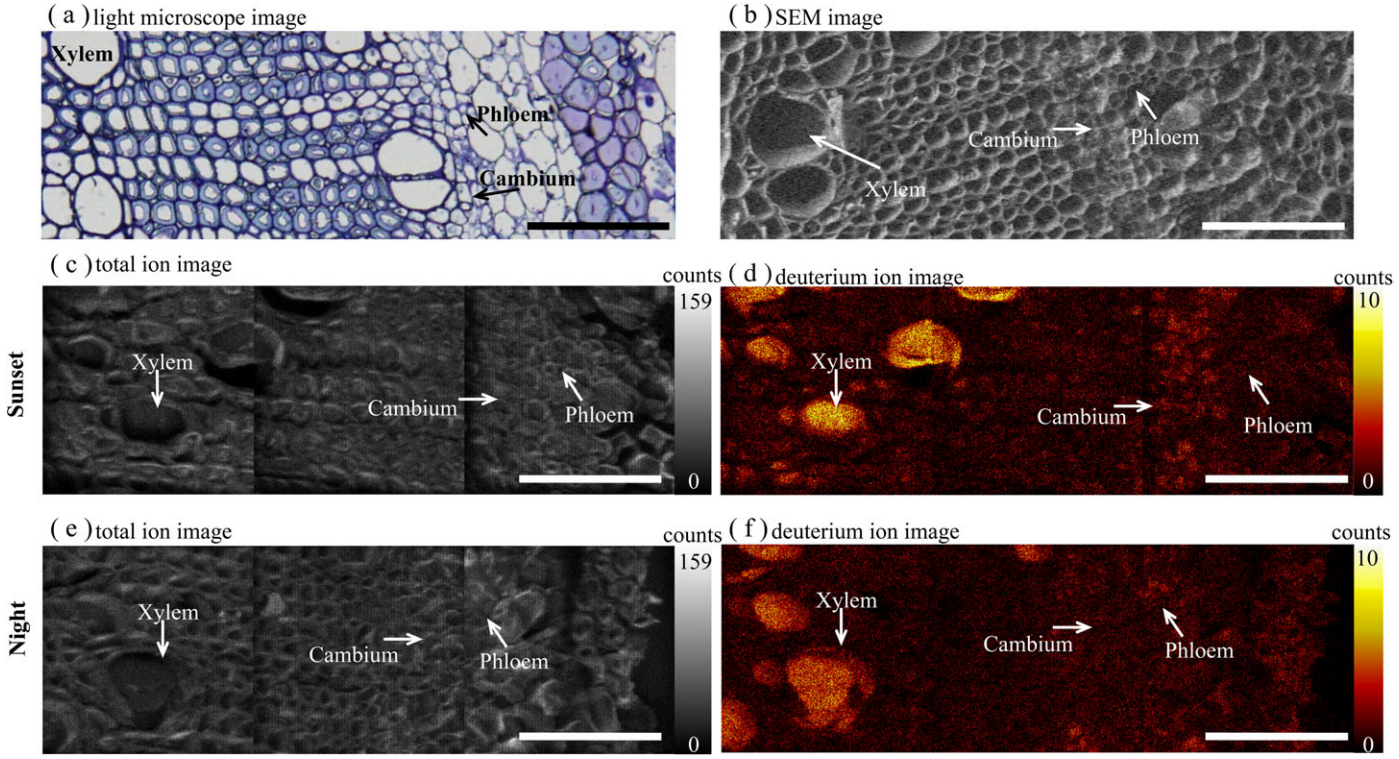

Fig. 5. Distribution of D_2O in soybean stem tissue under less (sampling during the sunset period; c and d) and no (sampling during the night period; e and f) evaporative demand (experiment 2). The specific resolution of ToF-SIMS images is 1.8 μm (three pixel step size). Scale bar (lower right in each figure)=100 μm. The coloured bars (right side) indicate the intensity of secondary ions. Black indicates the lowest intensity and white indicates the highest intensity.

Table 1. Comparison of deuterium ion counts (μm^{-2}) of each tissue under high (during the day), less (sunset) and no (night period) evaporative demand

D_2O labelling was done for 1 h during a sunny morning (9:00–10:00 h) inside an open glasshouse for high evaporative demand in experiment 1. In experiment 2, D_2O labelling was done for 4 h (13:00–17:00 h for sunset sampling) and 8 h (13:00–21:00 h for night sampling) in a growth chamber. The values are expressed as the average number of deuterium ion counts per 1 μm^2 of cells in each tissue. The control shows the mean of each tissue with unlabelled H_2O.

	Vessel		Cortex	Cambium	Parenchyma		Control
	Xylem	Phloem			Xylem	Phloem	
Day	8.04±0.56 a	4.65±0.45 b	4.32±0.40 b	4.05±0.44 b	1.25±0.07 c	0.89±0.07 c	
Sunset	13.61±0.79 a	1.94±0.22 c		4.33±0.56 b	1.45±0.08 c	1.65±0.13 c	0.13±0.02
Night	13.25±0.27 a	2.87±0.37 b		3.64±0.47 b	1.60±0.11 c	1.78±0.14 c	

Each value is shown as the average ±SE. The same letter within each row indicates no significant statistical difference at the 5% level by Fisher's PLSD with 4–8 replicate measurements.

demand is high. Although transpiration rates were not measured in this experiment, relatively high transpiration should have occurred in the plants under strong natural sunlight and ventilated air conditions. The transpirational pull may be so strong that the xylem water was not directly supplied to the stem parenchyma cells near the roots.

Under high evaporative conditions the growth of stem parenchyma cells would be minimal, and perhaps the stem parenchyma cells would hardly act as sinks. In contrast, during low or no evaporative demand these stem parenchyma cells would actively grow and will act as water sinks. The deuterium ion counts in the phloem complex were not higher than those in cambium under both less (sunset) and no (night) evaporative demand (Table 1). These results indicated that under less or no evaporative demand xylem water would be directly supplied to growing cells not via the phloem tissue. Sunset harvesting (deuterium labelling from 13:00 h to 17:00 h) even showed statistically lower ion counts in phloem than in cambium. The soybean cultivar used in this experiment usually showed lower photosynthetic and transpiration rates after 14:00–15:00 h (data not shown). At around sunset just before 17:00 h quite less transpiration probably occurs. Under such conditions, deuterium supply to the phloem may gradually cease. Absorbed deuterated water in xylem would gradually move to growing cells following the water potential gradient under less evaporative demand; higher in xylem and lower in xylem parenchyma to cambium tissues. During the afternoon hours cambium cells would actively grow, and therefore they would require a lot of water for the cell expansion growth. Enhanced deuterium accumulation in the cambium region in Fig. 5d would most probably indicate the higher water sink activity of these cells. In phloem tissues, the deuterium accumulation was significantly higher during the night than at sunset (*F*-test, $P < 0.05$). This indicated that the deuterium ions in phloem tissues located in the stem gradually increased during the night period compared with sunset hours. This may be attributed to the water movement from the xylem to the phloem in the leaf after stomatal closure. These results provided the visual and circumstantial evidence of water movement during the day and night period; xylem water would be supplied to the stem parenchyma cells in the stem via the phloem during high evaporative demand but it would be directly supplied to the growing cells during less or no evaporative demand.

Limitation of the present technique

Matrix effects in studies of plant tissue and/or the cellular level of analysis have not been discussed in depth so far, except for by Metzner *et al.* (2008). These authors stated that the use of isotopes overcomes the problem of matrix effects because the ratios of the isotopes are the basis for detection and quantification, thus allowing quantification of the tracer fraction. In the present study, materials of soybean stem tissue within the cellular level of observation should be more or less similar, and thus the matrix effects may be quite small in the case of the quantification of stable isotope. In fact Metzner *et al.* (2010) also used D_2O as the water tracer to observe the lateral exchange of water between xylem and surrounding tissues by the cryo-Tof-SIMS analysis. The detection limits for stable isotope tracers depend on the precision and standard deviation of the isotopic abundance measurements (Metzner *et al.*, 2010). Although the detection limits were not measured in the present study, this will not affect the measurement judging from the results of Metzner *et al.* (2010). The result of Metzner *et al.* (2010) indicated that the water tracer was equilibrated within minutes across the entire cross-section. They used climbing bean (*Phaseolus vulgaris* L.), and the water tracer was supplied from the cut end of the stem base. The reason for the discrepancy in the present results regarding water movement from xylem to stem parenchyma cells is not known at the moment. Most probably the difference in the method of water application may cause the different view of water movement. Further experimental evidence is required to determine the reason for the difference between the results.

Plunging actively transpiring plants into liquid nitrogen is likely to cause xylem cavitation (Cochard *et al.*, 2000). Hence, the possibility of an artificial influence should be

considered to explain the observed phenomenon. If cavitation occurs significantly in the present experiment, the image of deuterium distribution in xylem vessels should be regarded as a partially artefactual product. Even though xylem cavitation occurs, the deuterium ion density in each tissue should not be modified. Thus it will not affect the quantification of the deuterium density. Moreover, anatomical observation after the TOF-SIMS analysis was not easy with the TRIFT III used here. The technique should be modified in future to analyse the same sections for both deuterium concentration and anatomical survey following the progress of the cryo-system of Tof-SIMS.

Future implications

The present technique of tracing water movement by the use of a Tof-SIMS cryo-system will enable simultaneous evaluation of the water both inside the vascular cylinder and inside the parenchyma cells, at a high resolution cellular level. This technique can be used to quantify water movement in both symplastic and apoplastic pathways. This may contribute to validating the Munch pressure–flow hypothesis, which is not yet resolved (see, for example, Mullendore *et al.*, 2010). Moreover, this technique could even be used to analyse the water movement between soil and plants through the observation of root cap mucilage (Iijima *et al.*, 2003, 2008), the dynamic interface between plant and soil.

Acknowledgements

This study was funded by a grant-in-aid for exploratory research (19658006) from the Japan Society for the Promotion of Science.

References

Araki H, Iijima M. 2005. Stable isotope analysis of water extraction from subsoil in upland rice (*Oryza sativa* L.) as affected by drought and soil compaction. *Plant and Soil* **270,** 147–157.

Cochard H, Bodet C, Améglio T, Cruiziat P. 2000. Cryo-scanning electron microscopy observations of vessel content during transpiration in walnut petioles. Facts or artifacts? *Plant Physiology* **124,** 1191–1202.

Helfter C, Shephard JD, Martínez-Vilalta J, Mencuccini M, Hand DP. 2007. A noninvasive optical system for the measurement of xylem and phloem sap flow in woody plants of small stem size. *Tree Physiology* **27,** 169–179.

Higuchi H, Sakuratani T. 2006. Water dynamics in mango (*Mangifera indica* L.) fruit during the young and mature fruit seasons as measured by the stem heat balance method. *Journal of the Japanese Society for Horticultural Science* **75,** 11–19.

Hölttä T, Vesala T, Perämäki M, Nikinmaa E. 2006*a*. Refilling of embolised conduits as a consequence of 'Münch water' circulation. *Functional Plant Biology* **33,** 949–959.

Hölttä T, Vesala T, Sevanto S, Perämäki M, Nikinmaa E. 2006*b*. Modeling xylem and phloem water flows in trees according to cohesion theory and Münch hypothesis. *Trees* **20,** 67–78.

Iijima M, Asai T, Zegada-Lizarazu W, Nakajima Y, Hamada H. 2005. Productivity and water source of intercropped wheat and rice in a direct-sown sequential cropping system: the effects of no-tillage and drought. *Plant Production Science* **8,** 368–374.

Iijima M, Higuchi T, Barlow PW, Bengough AG. 2003. Root cap removal increases root penetration resistance in maize (*Zea mays* L.). *Journal of Experimental Botany* **54,** 2105–2109.

Iijima M, Morita S, Barlow PW. 2008. Structure and function of the root cap. *Plant Production Science* **11,** 17–27.

Iijima M, Morita A, Zegada-Lizarazu W, Izumi Y. 2007. No-tillage enhanced the dependence on surface irrigation water in wheat and soybean. *Plant Production Science* **10,** 182–188.

Imai T, Tanabe K, Kato T, Fukushima K. 2005. Localization of ferruginol, a diterpene phenol, in *Cryptomeria japonica* heartwood by time-of-flight secondary ion mass spectrometry. *Planta* **221,** 549–556.

Keller M, Smith JP, Bondada BR. 2006. Ripening grape berries remain hydraulically connected to the shoot. *Journal of Experimental Botany* **57,** 2577–2587.

Köckenberger W, De Panfilis C, Santoro D, Dahiya P, Rawsthorne S. 2004. High resolution NMR microscopy of plants and fungi. *Journal of Microscopy* **214,** 182–189.

Liu Z, Gaskin RE. 2004. Visualisation of the uptake of two model xenobiotics into bean leaves by confocal laser scanning microscopy: diffusion pathways and implication in phloem translocation. *Pest Management Science* **60,** 434–439.

Matsushita Y, Ookura A, Imai T, Fukushima K, Kato T. 2005. Analysis of behavior of rosin glycerin ester in rosin ester emulsion size by visualization using ToF-SIMS. *Japan Tappi Journal* **59,** 1685–1693.

Matsushita Y, Sekiguchi T, Saito K, Kato T, Imai T, Fukishima K. 2007. The characteristic fragment ions and visualization of cationic starches on pulp fiber using ToF-SIMS. *Surface and Interface Analysis* **39,** 501–505.

Metzner R, Schneider HU, Breuer U, Schroeder WH. 2008. Imaging nutrient distributions in plant tissue using time-of-flight secondary ion mass spectrometry and scanning electron microscopy. *Plant Physiology* **147,** 1774–1787.

Metzner R, Thorpe MR, Breuer U, Blumler P, Schurr U, Heike U, Schneider HU, Schroeder WH. 2010. Contrasting dynamics of water and mineral nutrients in stems shown by stable isotope tracers and cryo-SIMS. *Plant, Cell and Environment* **33,** 1393–1407.

Mullendore DL, Windt CW, Van As H, Knoblauch M. 2010. Sieve tube geometry in relation to phloem flow. *The Plant Cell* **22,** 579–593.

Münch E. 1930. *Die Stoffbewegungen in der Pflanze. Jena,* Germany: Fisher.

Nair AP, Tyler BJ, Peterson RE. 2004. Application of a cryo-stage in the TOF-SIMS analysis of atmospheric aerosol surfaces. *Applied Surface Science* **231–232,** 538–542.

Nakanishi TM, Okuni Y, Furukawa J, Tanoi K, Yokota H, Ikeue N, Matsubayashi M, Uchida H, Tsuji A. 2003. Water movement in a plant sample by neutron beam analysis as well as positron emission tracer imaging system. *Journal of Radioanalytical and Nuclear Chemistry* **255,** 149–153.

Peuke AD, Windt C, Van As H. 2006. Effects of cold-girdling on flows in the transport phloem in *Ricinus communis*: is mass flow inhibited? *Plant, Cell and Environment* **29,** 15–25.

Saito K, Kato T, Takamori H, Kishimoto T, Fukushima K. 2005*a*. A new analysis of the depolymerized fragments of lignin polymer using ToF-SIMS. *Biomacromolecules* **6,** 2688–2696.

Saito K, Kato T, Takamori H, Kishimoto T, Yamamoto A, Fukushima K. 2006. A new analysis of the depolymerized fragments of lignin polymer in the plant cell walls using ToF-SIMS. *Applied Surface Science* **252,** 6734–3737.

Saito K, Kato T, Tsuji Y, Fukushima K. 2005*b*. Identifying the characteristic secondary ions of lignin polymer using ToF-SIMS. *Biomacromolecules* **6,** 678–683.

Sano Y, Okamura Y, Utsumi Y. 2005. Visualizing water-conduction pathways of living trees: selection of dyes and tissue preparation methods. *Tree Physiology* **25,** 269–275.

Scheenen TWJ, Vergeldt FJ, Heemskerk AM, Van As H. 2007. Intact plant magnetic resonance imaging to study dynamics in long-distance sap flow and flow-conducting surface area. *Plant Physiology* **144,** 1157–1165.

Schneider H, Manz B, Westhoff M, *et al*. 2003. The impact of lipid distribution, composition and mobility on xylem water refilling of the resurrection plant *Myrothamnus flabellifolia*. *New Phytologist* **159,** 487–505.

Sibgatullin TA, Vergeldt FJ, Gerkema E, Van As H. 2010. Quantitative permeability imaging of plant tissues. *European Biophysics Journal* **39,** 699–710.

Tokareva EN, Pranovich AV, Fardim P, Daniel G, Holmbom B. 2007. Analysis of wood tissues by time-of-flight secondary ion mass spectrometry. *Holzforschung* **61,** 647–655.

Van As H. 2007. Intact plant MRI for the study of cell water relations, membrane permeability, cell-to-cell and long-distance water transport. *Journal of Experimental Botany* **58,** 743–756.

Varney GT, Canny MJ. 1993. Rates of water uptake into the mature root system of maize plants. *New Phytologist* **123,** 775–786.

Varney GT, McCully ME, Canny MJ. 1993. Sites of entry of water into the symplast of maize roots. *New Phytologist* **125,** 733–741.

Windt CW, Vergeldt FJ, Jager PA, Van As H. 2006. MRI of long-distance water transport: a comparison of the phloem and xylem flow characteristics and dynamics in poplar, castor bean, tomato and tobacco. *Plant, Cell and Environment* **29,** 1715–1729.

Windt CW, Vergeldt FJ, Van As H. 2007. Correlated displacement—T_2MRI by means of a pulsed field gradient multi-spin echo method. *Journal of Magnetic Resonance* **185,** 230–239.

Zegada-Lizarazu W, Iijima M. 2004. Hydrogen stable isotope analysis of water acquisition abilities of deep roots and hydraulic lift in sixteen food crop species. *Plant Production Science* **7,** 427–434.

Zegada-Lizarazu W, Iijima M. 2005. Deep root water uptake and water use efficiency of pearl millet in comparison to other millet species. *Plant Production Science* **8,** 454–460.

Zegada-Lizarazu W, Izumi Y, Iijima M. 2006*a*. Water competition of intercropped pearl millet with cowpea under drought and soil compaction stresses. *Plant Production Science* **9,** 123–132.

Zegada-Lizarazu W, Kanyomeka L, Izumi Y, Iijima M. 2006*b*. Pearl millet developed deep roots and changed water sources by competition with intercropped cowpea in the semiarid environment of northern Namibia. *Plant Production Science* **9,** 355–363.

Zegada-Lizarazu W, Kanyomeka L, Izumi Y, Iijima M. 2007. Water acquisition from the seasonal wetland and root development of the intercropped pearl millet in flooding ecosystem of northern Namibia. *Plant Production Science* **10,** 20–27.

Zegada-Lizarazu W, Niitembu S, Iijima M. 2005. Mixed planting modified the water source and water use of pearl millet. *Plant Production Science* **8,** 433–440.